Title
An on-chip microfluidic pressure regulator that facilitates reproducible loading of cells and hydrogels into microphysiological system platforms

Journal
Lab on a Chip, 16(5)

ISSN
1473-0197

Authors
Wang, Xiaolin
Phan, Duc TT
Zhao, Da
et al.

Publication Date
2016-03-07

DOI
10.1039/c5lc01563d

Peer reviewed

HHS Public Access

Author manuscript

Lab Chip. Author manuscript; available in PMC 2017 March 07.

Published in final edited form as:

Lab Chip. 2016 March 07; 16(5): 868–876. doi:10.1039/c5lc01563d.

An on-chip microfluidic pressure regulator that facilitates reproducible loading of cells and hydrogels into microphysiological system platforms

Xiaolin Wang[a], **Duc T. T. Phan**[b], **Da Zhao**[a], **Steven C. George**[c], **Christopher C. W. Hughes**[#a,b,d], and **Abraham P. Lee**[#a,e]

[a]Department of Biomedical Engineering, University of California, Irvine, CA 92697, USA.

[b]Department of Molecular Biology and Biochemistry, University of California, Irvine, CA 92697, USA.

[c]Department of Biomedical Engineering, Washington University in St. Louis, Saint Louis, MO 63130, USA.

[d]Edwards Lifesciences Center for Advanced Cardiovascular Technology, University of California, Irvine, CA 92697, USA.

[e]Department of Mechanical and Aerospace Engineering, University of California, Irvine, CA 92697, USA.

[#] These authors contributed equally to this work.

Abstract

Coculturing multiple cell types together in 3-dimensional (3D) cultures better mimics the *in vivo* microphysiological environment, and has become widely adopted in recent years with the development of organ-on-chip systems. However, a bottleneck in set-up of these devices arises as a result of the delivery of the gel into the microfluidic chip being sensitive to pressure fluctuations, making gel confinement at a specific region challenging, especially when manual operation is performed. In this paper, we present a novel design of an on-chip regulator module with pressure-releasing safety microvalves that can facilitate stable gel delivery into designated microchannel regions while maintaining well-controlled, non-bursting gel interfaces. This pressure regulator design can be integrated into different microfluidic chip designs and is compatible with a wide variety of gel injection apparatuses operated automatically or manually at different flow rates. The sensitivity and working range of this pressure regulator can be adjusted by changing the width of its pressure releasing safety microvalve design. The effectiveness of the design is validated by its incorporation into a microfluidic platform we have developed for generating 3D vascularized micro-organs (VMOs). Reproducible gel loading is demonstrated for both an automatic syringe pump and a manually-operated micropipettor. This design allows for rapid and reproducible loading of hydrogels into microfluidic devices without the risk of bursting gel-air interfaces.

aplee@uci.edu; Fax: +1(949)824-1727; Tel: +1(949)824-9691.
cchughes@uci.edu; Fax: +1 (949) 824-8551; Tel: +1 (949)824-8771.

Introduction

In recent years, 3D cell culture models have attracted much attention because they can better mimic the *in vivo* microphysiological environment by incorporating various cell types into hydrogels, including native extracellular matrices (ECM), for long-term cell culture [1]. By integrating 3D hydrogels into microfluidic chips, additional parameters of the microenvironment such as dynamic mechanical cues (e.g. fluid shear stress, interstitial fluid flow, etc.) or spatiotemporal chemical gradients (e.g. growth factor gradients) can be precisely controlled [2]. These sophisticated microfluidic cell culture systems can facilitate the formation of 3D microtissues with specific physiological functions such that we are now beginning to create “organ-on-a-chip” models [3-5].

In order to provide an avenue for cells to access nutrients and oxygen as well as for waste removal, development of perfusion-based 3D cell cultures with physiological flow through tissue interstitial space has become critical [6-8]. The most commonly used method is to establish fluid flow by setting up two microfluidic channels adjacent to a tissue chamber seeded with cell-ECM suspension [9-11]. In this geometry it is critical that the cell-ECM mixture be confined inside the tissue chamber without leaking into the adjacent microfluidic channels, which would lead to flow obstruction. Conversely, the contact surface between the fluid inside the microfluidic channel and the cell-ECM suspension inside the tissue chamber should be sufficient for biotransportation across the microtissue. Although micro-pillar arrays and other microstructures functioning as microvalves can prevent gel bursting to a certain extent [12, 13], operation failure often occurs due to internal pressure transients exceeding the burst pressure of the air-cell/ECM interface during loading. Use of a syringe pump, where the dispensed volume and the applied flow rate can be more finely controlled, can improve reproducibility over manual loading, however, it is cumbersome to connect the syringe with each microfluidic chip via tubing, and bubbles may easily be generated when connecting and removing tubing, making it undesirable for high-throughput applications. In addition, gel loading with syringe pumps is unsuitable for certain hydrogels that require rapid mixing with a catalytic reagent to fully polymerize. Due to their flexible and easy operation micropipettors are the preferred alternative for hydrogel loading. However, with manual operation it is difficult to achieve constant and consistent flow rates, resulting in pressure fluctuations and gel bursting.

In this paper, we present a novel design of an on-chip regulator module with pressure releasing safety microvalves that can effectively maintain the hydraulic pressure inside the gel loading channel within a specified range. The power of this module is validated by its incorporation into a microfluidic platform for culturing 3D vascularized micro-organs (3D-VMO). Using this microfluidic platform we tested both automatic gel loading using a syringe pump and manual gel loading using a micropipettor. These tests demonstrated the module's compatibility with different liquid handling systems and its flexibility to operate in either automatic or manual mode. Experimental results show that the on-chip pressure regulator facilitates robust gel loading into the tissue chamber under multiple different flow rates without bursting into the adjacent microfluidic channels. Finally, the sensitivity and working range of the pressure regulator can be fine-tuned by adjusting the width of the

safety microvalves relative to the air-gel interface width. The simplicity of the design allows for easy integration into any microfluidic chip that requires loading of hydrogels.

Materials and methods

Pressure regulator module design

As shown in Fig. 1A, the on-chip pressure regulator module consists of pressure-releasing capillary burst valves (denoted as *safety microvalves*) and diversion channels, all based on three basic design principles. First, the burst pressure of safety microvalves in the pressure regulator module should be lower than that of the tissue chamber capillary burst valves (denoted as *perfusion microvalves*) used for confining loaded gel inside the tissue chambers. This ensures that the safety microvalves will burst first to release redundant gel and regulate the pressure inside the tissue chambers to below the burst pressure of perfusion microvalves. Second, in order to redirect the redundant gel away from the tissue chambers, the pressure regulator module should be positioned upstream of the gel loading channel. Third, the volume of storage space to accommodate the redundant gel should be large enough for a typical single injection volume.

Figure 1B shows integration of the pressure regulator module design into a perfusion-based microfluidic device for 3D-VMO. The chip design consists of one gel loading channel with three central mm-sized diamond tissue chambers (1×2 mm), each connected to two adjacent microfluidic channels (width: 100 μm) through capillary burst valves (perfusion microvalves, width: 50 μm) that confine the loaded gel inside the tissue chambers [14, 15]. The pressure regulator module consists of two capillary burst valves (safety microvalves, width: 65 μm) directly connected to the gel loading channel and positioned between the gel loading inlet and the first tissue chamber. A wide microfluidic channel (width: 300 μm) as the diversion channel was utilized to redirect and accommodate the redundant gel. The microfluidic features throughout the device had a constant height of 100 μm.

The entire device can be simulated by a simplified electronic circuit model [16, 17], as shown in Fig. 1C. The external pressure source (P_{in}) connected to the inlet of the gel loading channel is analogous to a DC voltage source, and the outlet of the gel loading channel can be treated as the floating ground (GND), since it is open to the atmosphere (P_{atm}). The electrical resistance is analogous to the corresponding hydraulic resistance, which can be determined by the channel geometry and dimension. The backward diode represents the capillary burst valve, and its breakdown level corresponds to the burst pressure that varies inversely with the microvalve width. Correspondingly, the maximum backward voltage of D_1 (safety microvalve: 65 μm) was smaller than that of D_2 (perfusion microvalve: 50 μm). Once the diode breaks down, it would no longer prevent the reverse current, which is analogous to gel bursting. The capacitor C represents the diversion channel to release and accommodate the redundant gel, and its capacitor volume corresponds to the designed volume of this diversion channel.

Figure 1D shows simulation results for the gel loading process in both the tissue chamber and the pressure regulator module. The “Two-Phase Flow, Laminar, Level Set” application mode in the MEMS module of COMSOL Multiphysics (COMSOL, Burlington, MA) was

utilized to simulate the moving interface of two immiscible fluid flows by solving the Navier-Stokes equation. The Navier-Stokes equation describes the transport of mass and momentum for fluids with constant density, incorporating surface tension and conservation of mass. The “Level Set” method was utilized to predict the moving interface by using the smooth signed distance function, denoted as ϕ (In air ϕ=0, in gel ϕ=1, and at interface ϕ=0.5). Therefore, the “Level Set” function can be thought of as the volume fraction of gel during the loading process. In the COMSOL simulation, two consecutive computations were executed. First, a smooth initial condition for the “Level Set” variable was calculated, and the solution was stored. Then the transient analysis was started for the time-dependent simulation of fluid motion. The contact angle between the wall and the gel interface as well as the microvalve dimensions were key variables that controlled the gel filling process. Since the inner surface of microfluidic channel made from poly(dimethylsiloxane) (PDMS) is hydrophobic, the injected gel will be confined inside the gel loading channel without bursting into the adjacent microfluidic channels or the diversion channel if the applied hydraulic pressure inside the tissue chambers and pressure regulator module is less than the burst pressure of their corresponding microvalves. Even though the gel precursor viscosity as an important variable contributes to the gel filling speed (fluid motion) during the loading process, the novel pressure regulator module design with high versatility will work for different hydrogel loading regardless of their precursor viscosities.

Gel loading model simplification

The gel loading process usually consists of two stages: the gel moving from inlet to outlet uniformly along the gel loading channel with the same height (S1), and the accumulation of redundant gel at the outlet reservoir (S2), as shown in Fig. 2A. Assuming incompressible laminar flow inside the microfluidic channel, the pressure drop ΔP across the gel loading channel is determined by the product of volume flow rate Q and the fluidic resistance R of the channel (Poiseuille's flow), which is described as [18]:

$$\Delta P = Q * R \quad (1)$$

For the first stage (S1), since the gel is fully distributed along the gel loading channel, its fluidic resistance $R_{channel}$ is solely determined by the channel geometry (i.e. width, height, and whole channel length). Therefore, equation (1) can be expressed as:

$$\Delta P_{S1} = P_{injection} - P_{air} = Q * R_{channel} \quad (2)$$

where $P_{injection}$ is the pressure applied at the gel loading inlet, and P_{air} is the atmosphere pressure.

However, at the second stage (S2), since there is a certain height of gel accumulated at the outlet reservoir, which can be simplified as an extended channel, the total fluidic resistance of the gel loading channel will increase accordingly. With the increased gel height at the outlet reservoir, the cross section of extended channel with fixed length will become narrow accordingly due to the increased fluidic resistance. Therefore, be simplified as an extended

channel, the total fluidic resistance of the gel loading channel will increase accordingly. With the increased gel height at the outlet reservoir, the cross section of extended channel with fixed length will become narrow accordingly due to the increased fluidic resistance. Therefore, the pressure drop along the gel loading channel during the second stage can be expressed as:

$$\Delta P_{S2} = P_{injection} - P_{air} = Q * (R_{channel} + R_{extended}) \quad (3)$$

where $R_{extended}$ is the fluidic resistance of the extended channel.

Therefore, the pressure inside the gel loading channel will build up abruptly as a result of either the high flow rate applied at the first stage (S1), or the dramatically increased fluidic resistance at the second stage (S2). When the internal hydraulic pressure exceeds the burst pressure of microvalves, gel leakage or bursting will occur.

Burst pressure at designed microvalves

To better understand the gel transversing process, it is necessary to characterize the pressure difference exerted on the gel-air interface during the loading process, which can be analyzed by the Young-Laplace equation expressed as [19]:

$$P_{gel} - P_{air} = -2\gamma (\cos\theta_s / w + \cos\theta_v / h) \quad (4)$$

where P_{gel} is the gel pressure inside the interface, γ is surface tension, w and h are width and height of the microfluidic channel where the interface is located, θ_s is the contact angle formed between the gel interface and sidewalls, and θ_v is the contact angle of gel interface with the top wall and bottom wall. Therefore, for a given gel with fixed surface tension, the pressure difference across the interface can be adjusted by changing either the microfluidic channel dimensions or the interface curvature with different contact angles.

If the contact angles with all sidewalls exceed the critical advancing contact angle θ_A (i.e. $\theta_s \geq \theta_A$ and $\theta_v \geq \theta_A$), the interface will burst to induce gel movement, as shown in Fig. 2B. When the gel meniscus is in motion with sufficiently low contact line velocity U and small capillary number $Ca = \mu U/g < 10^{-3}$, where μ is the gel viscosity, we can set its dynamic contact angle $\theta_s \approx \theta_v \approx \theta_A$. Therefore, the pressure difference for the gel bursting interface can be described as:

$$P_{gel-burst} - P_{air} = -2\gamma (\cos\theta_A / w + \cos\theta_A / h) \quad (5)$$

Due to its single-use feature and simple structure for microfabrication, capillary burst valves are ideal candidates for both safety microvalves at the pressure regulator module and perfusion microvalves at the tissue chambers. Capillary burst valves are characterized by the abrupt change of fluid contact angle to form the high energy meniscus. The increased capillary resistance can be accomplished by the abrupt change of either channel geometry or

surface chemistry [13]. For geometrical capillary burst valves, a sudden diverging section of microstructure is normally designed to trap the gel meniscus at the point of expansion. As shown in Fig. 2C, the expanded external sidewall with gentle slope is utilized as the capillary burst valve in our design. When the meniscus approaches the external sidewall, its contact angle reduces from θ_A to $\theta_s^*=\theta_A - \beta$, where β is the angle between the internal sidewall and the external sidewall, thus the gel stops instantly. The gel interface will bulge gradually as the pressure builds up, until its contact angle with the external sidewall increases to θ_A, which also means that the contact angle with the internal sidewall increases up to $\theta_A^*=\theta_A + \beta$. It is noted that the maximum contact angle for a liquid meniscus cannot exceed 180°, thus the critical bursting contact angle with the internal sidewall for the capillary burst valve should be $\theta_A^*=\min\{\theta_A + \beta, 180°\}$. Therefore, the burst pressure for our designed microvalves $P_{valve\text{-}burst}$ can be expressed as:

$$P_{valve-burst} - P_{air} = -2\gamma\left(\cos\theta_A^*/w + \cos\theta_A/h\right) \quad (6)$$

Gel interface control at the perfusion microvalve

Based on the relative relationship between the applied gel injection pressure and the Laplace pressure of the gel-air interface, the loaded gel can be directed to different locations of the perfusion microvalve with different interface curvatures (Fig. S1). For certain applications, it is necessary to confine the gel at a specific location with a well-controlled gel interface curvature. For example, a relatively flat gel interface is required for an endothelial cell monolayer to mimic a vessel wall [15, 20]. With the addition of the pressure regulator module, it is possible to control the specific gel interface curvature positioned at the perfusion microvalve by designing a corresponding safety microvalve with a certain width.

Based on Young-Laplace equation, when gel bursting occurred at the safety microvalve, its burst pressure should be equal to the Laplace pressure at the perfusion microvalve with specific gel interface curvature. If these two valves were close enough, it could be formulated as:

$$\frac{\cos\theta^*_{A-safety}}{w_{safety}} = \frac{\cos\theta'_{s-perfusion}}{w_{perfusion}} \left(\theta_{A-perfusion} \le \theta'_{s-perfusion} < \theta^*_{A-perfusion}\right) \quad (7)$$

where $\theta^*_{A\text{-}safety}$ and $\theta^*_{A\text{-}perfusion}$ are the critical bursting contact angles with the internal sidewall for safety microvalve and perfusion microvalve respectively, $\theta_{A\text{-}perfusion}$ is the critical advancing contact angle with the internal sidewall for the perfusion microvalve, $\theta'_{s\text{-}perfusion}$ is the contact angle with the internal sidewall for the perfusion microvalve, and w_{safety} and $w_{perfusion}$ are the widths of the safety microvalve and the perfusion microvalve, respectively. If the gel with a relatively flat interface (i.e. $\theta'_{s\text{-}perfusion} = \theta_{A\text{-}perfusion}$) is desired at the perfusion microvalve, the width of safety microvalve could be calculated by:

$$w_{safety} = \frac{\cos \theta^*_{A-safety}}{\cos \theta_{A-perfusion}} w_{perfusion} \quad (8)$$

Cell culture

For cell culture, human endothelial colony forming cell-derived endothelial cells (hECFC-ECs) were obtained from cord blood as previously described [21]. hECFC-ECs were selected and expanded on flasks coated with 10 μg/mL fibronectin (Sigma Aldrich) in EGM-2 (Lonza) and transduced with mCherry-expressing lentiviral construct (LeGO-C2/ Addgene plasmid: 27339) to express fluorescence. Normal human lung fibroblasts (NHLF) were purchased from Lonza and expanded in 10% FBS DMEM (Corning). hECFC-ECs and NHLFs were used for experiments between passage 4 and 9 and cultured in a 37°C, 5% CO2, and 20% O2 incubator in 100% humidified air. Experimental set up for VMO in microfluidic platform was performed as previously described [15]. All experimental procedures were performed inside a Biosafety Level 2 laminar flow hood with sterile techniques.

Results and discussion

Performance of the pressure regulator under different flow rates

We first tested the performance of the pressure regulator module by automatic dye-mixed gel loading with a syringe pump under different flow rates, as shown in Fig. 3 and supplemental movie clip (ESI † Movie S1). In order to position the loaded gel at vertices of the perfusion microvalves with a non-bursting, relatively flat interface, the width of the safety microvalve (w_{safety}) was designed to be 65 μm by assuming $\theta^*_{A\text{-}safety}$=180°, $\theta_{A\text{-}perfusion}$=140°, and $w_{perfusion}$ =50 μm. Therefore, the calculated burst pressure for the safety microvalve and the perfusion microvalve are 3318 Pa and 3983 Pa respectively (surface tension of water γ=0.072 N m^{-1}). As shown in Fig. 3A, when the applied flow rate was less than 90μL/min, no gel bursting occurred at the safety microvalves of the pressure regulator module during the first stage (S1-B0). However, at the second stage, the hydraulic pressure inside the gel loading channel gradually built up with the increased fluidic resistance at the outlet reservoir. Once the hydraulic pressure surpassed the burst pressure of the safety microvalve, gel burst into one (S2-B1) or two (S2-B2) diversion channels to release the redundant gel. When the applied flow rate was higher than 170μL/min, although the fluidic resistance remains constant during the first stage, gel bursting from one safety microvalve still occurred due to the high flow rate (S1-B1). At the second stage, the other safety microvalve also burst to release the built-up pressure resulting from the increased fluidic resistance. In all these cases, the gel interface at the perfusion microvalves maintained a relatively flat profile. However, when the applied flow rate was high (e.g. 320μL/min), both safety microvalves burst during the first stage (S1-B2), which makes them no longer available to accommodate the second stage. To resolve this issue, a narrower (e.g. 55 μm or less) safety microvalve could be integrated into the pressure regulator module design. Figure S2 in supplementary

†Electronic Supplementary Information (ESI) available: See DOI: 10.1039/x0xx00000x.

material shows more detailed information on the hydraulic pressure profile inside the gel loading channel at different stages under different flow rates. A control experiment was conducted by using the same gel loading channel without the pressure regulator module. As shown in Fig. 3B, when the applied flow rate was over 150μL/min, the gel interface at the perfusion microvalves bulged until it finally burst into one or two adjacent microfludic channels.

Sensitivity and working range for the pressure regulator

Figure 4A and a supplemental movie clip (ESI † Movie S2) show the dye-mixed gel loading performance with either 55μm or 85μm wide safety microvalves under different flow rates, respectively. In the device with the 85μm wide safety microvalve, one safety microvalve burst to release pressure at the second stage under a flow rate as low as 50μL/min (S1-B0, S2-B1). At the same flow rate, both 55μm wide safety microvalves were intact. The upper limit of the range for the 85μm wide safety microvalve was 130μL/min (S1-B1, S2-B2). In contrast, the 55μm wide safety microvalve was activated when the applied flow rate was increased to 100μL/min and its working limit was as high as 320μL/min.

Thus, the sensitivity and working range for the pressure regulator module can be flexibly adjusted by the width of the safety microvalves. Figure 4B showed the comparison results of the sensitivity and working range of safety microvalves with different widths, highlighting that the pressure regulator is more sensitive with wider safety microvalves. However, at the expense of sensitivity, the wor king range is inversely proportional to the microvalve width. Thus, there is a tradeoff between the sensitivity and working range for the pressure regulator module. Based on different needs and applications, either a narrow safety microvalve with large working range, or a wide safety microvalve with high sensitivity could be utilized. For example, if a well-controlled gel interface curvature is desired, the pressure regulator module should be sensitive enough to release the build-up pressure rapidly, but this also requires the injection apparatus to operate with high accuracy to maintain a constant flow rate. If injection equipment is used that exhibits a large pressure fluctuation during injection, or a manual injection mode is utilized, then the pressure regulator module with a large working range should be used to ensure robust gel loading without bursting.

Gel confinement using perfusion microvalves with wide openings

The width of the perfusion valve that connects the cell-containing gel matrix to the outer microfluidic channels (initially air-filled and then medium-filled) determines the rate at which biotransportation (convection) occurs across the gel. By integrating the pressure regulator module into the device it is possible to use wider perfusion microvalves while still retaining gel, thus allowing for greater rates of convection compared to narrower microvalves while maintaining the same hydrostatic pressure drop (Fig. S3). Figure 5 and a supplemental movie clip (ESI † Movie S3) show the gel loading performance using 100μm wide perfusion microvalves and 130μm wide safety microvalves at different flow rates. The pressure regulator module was activated at a flow rate of 45μL/min, and its upper limit was 70μL/min. In comparison with the 50μm wide perfusion microvalve, both the pressure regulator module and gel interface were sensitive to the change of applied flow rate. Once the flow rate was over 70μL/min, two pressure safety microvalves burst at the first stage (S1-

B2). An alternative method to prevent gel bursting from the perfusion microvalves with wide openings under high flow rates would be to prevent or reduce pressure build-up with the increased fluidic resistance at the second stage. This could be achieved by changing the dispensed gel volume, as shown in Figure 5. Here, only 10μL dye-mixed gel was injected when the flow rate was over 70μL/min. Because the fluidic resistance of the gel loading channel was less than that of the pressure regulator module, even though some gel was redirected into two diversion channels during the first stage, a large part of the injected gel flowed along the gel loading channel and filled up the tissue chambers. At a flow rate of 120μL/min, bursting of two safety microvalves occurred earlier than that at flow rate of 70μL/min during the first stage, but they were still able to prevent gel bursting into the adjacent microfluidic channels. If more volume of medium is needed to supply sufficient mass transfer to sustain the cells, one can increase either the number of perfusion microvalves connected to each tissue chamber or the hydraulic pressure drop across the tissue chambers.

Manual cell-seeded gel loading with a micropipettor

We further tested the performance of the pressure regulator module by manually loading the gel with a micropipettor. In this experiment we used our previously published VMO model to also confirm the biocompatibility of our design [15]. Human ECFC-ECs and NHLF were suspended in 10 mg/mL fibrinogen solution and then quickly mixed with 50U/mL thrombin for a final concentration of 3U/mL [22]. Since the polymerization time for fibrinogen after mixing with thrombin was short, it needed to be quickly injected into the gel loading channel. Therefore, it was difficult to operate the process fast enough using a syringe pump. Regardless of the pipetting speed manually applied to the micropipettor, the pressure regulator module effectively prevented gel bursting similar to the experimental results of dye-mixed gel loading with the syringe pump, as shown in Fig. 6A and a supplemental movie clip (ESI † Movie S4). When the slow pipetting speed was applied on push-button, no gel bursting occurred at the pressure regulator module. When the fast pipetting speed was applied, one or two safety microvalves burst to release the hydraulic pressure inside the tissue chambers to prevent gel bursting out of the perfusion microvalves. Figure 6B shows the successfully-formed 3D VMO after 7 days in culture in the microfluidic device using different loading force and bursting conditions.

Independent gel loading and microenvironment control of interconnected tissue chambers

There is considerable interest in connecting organ-on-chip modules (e.g. liver and gut for metabolic studies or colon and lung for metastasis studies), however, the mechanics of this are still being explored. Here we show that use of the pressure regulator module can facilitate heterotypic gel confinement inside a microfluidic device with interconnected structures (Fig. 7). A gel loading inlet and a pressure regulator module as gel loading outlet can be integrated at each end of the tissue chamber, allowing for individual loading of each compartment without bursting into the central connecting channel. The connecting channel can then be loaded at a later time to facilitate connection between the two halves (Fig. 7, S4). Our design differs from previously reported chip designs for heterotypic gel loading that cannot realize the independent microenvironment control [6, 11], and has the advantage of increased flexibility. Figure S5 shows that each tissue chamber can be separately loaded

with different particles mixed in the gel to mimic cells, and perfused with different liquid dyes, mimicking independent microenvironment control. This design can be used for multi-tissue co-culture, tumor angiogenesis, and human body-on-chip drug screening applications.

Discussion

By integrating a pressure regulator module into our microfluidic platform (3D-VMO model) we can effectively prevent gel bursting from the tissue chambers to the adjacent microfluidic channels. The device operates on a single microfluidic layer and maintains a well-controlled gel interface under different flow rates. This design has greatly facilitated reliable and reproducible loading of gels into the device as the steep learning curve required for successful manual loading is now obviated – any overpressure by the operator is efficiently suppressed as gel is diverted to the overflow to prevent bursting of the air-gel interface. The device also allows us to control the size and characteristics of the air-gel interface, which is critical for controlling the rate of convection, and is also important for applications requiring seeding of monolayer cells into the outer microfluidic channels.

For a multi-tissue communication device, two different hydrogels or the same hydrogel containing a different cell population need to be injected sequentially into the interconnected tissue chambers with independent microenvironment control. We have shown how this is possible using a modified design with the integration of pressure regulator module as gel loading outlet (Fig. 7). However, since the hydrogels inside each compartment are interconnected and become one unit, the fluidic resistance of the whole tissue chamber will increase greatly and this can affect the perfusion performance (e.g. interstitial flow velocity or profile, etc.) inside the tissue chamber [23]. In order to maintain uniform and well-controlled perfusion it might be beneficial to separate the fluidic channel and multi-tissue co-culture chambers into different layers. In this case it will be necessary to prevent the individual injected gel inside its respective tissue chamber from bursting both horizontally and vertically, which can also be realized with the assistance of pressure regulator module. Here, the safety microvalve burst pressure of the regulator module should be less than both the advancing pressure between different layers and the burst pressure between the interconnected tissue chambers in different rows.

Conclusion

In this paper, we present a novel on-chip pressure regulator module design that facilitates robust, reproducible, non-bursting hydrogel injection. The build-up pressure under different gel loading stages induced by redundant gel can be released by the activation of the pressure regulator module, once the hydraulic pressure inside the gel loading channel is higher than the safety microvalve burst pressure of the pressure regulator module. Furthermore, it can generate a well-controlled gel interface at a specific location in the perfusion microvalves under a wide range of flow rates. Due to its simple design, the pressure regulator module can be integrated into any microfluidic device that requires various types of hydrogel loading. In addition, both the sensitivity and working range of the pressure regulator module can be flexibly adjusted by changing the width of the safety microvalves according to specific applications. The pressure regulator module also allows for confining gels at perfusion microvalves with wide openings. Experiments on dye-mixed gel loading with a syringe

pump and cell-seeded gel loading with a micropipettor demonstrate the module's compatibility with versatile liquid handling apparatuses operated in either automatic or manual mode. The pressure regulator module design is versatile and enables designs that require placement of heterotypic tissue culture gels and microfluidic channels in different arrangements. It should prove useful for multi-organ-on-chip platforms.

Supplementary Material

Refer to Web version on PubMed Central for supplementary material.

Acknowledgements

This work was supported by grants from the National Institutes of Health: UH3 TR00048 and PQD5 CA180122. C. C. W. H. receives support from the Chao Family Comprehensive Cancer Center (CFCCC) through an NCI Center Grant award P30A062203.

References

1. Lee DH, Bae CY, Kwon S, Park JK. Lab Chip. 2015; 15(11):2379. [PubMed: 25857752]
2. Vickerman V, Blundo J, Chung S, Kamm R. Lab Chip. 2008; 8(9):1468. [PubMed: 18818801]
3. Chan CY, Huang P-H, Guo F, Ding X, Kapur V, Mai JD, Yuen PK, Huang TJ. Lab Chip. 2013; 13(24):4697. [PubMed: 24193241]
4. Bhatia SN, Ingber DE. Nat. Biotechnol. 2014; 32(8):760. [PubMed: 25093883]
5. Huh D, Torisawa YS, Kim HJ, Ingber DE. Lab Chip. 2012; 12(12):2156. [PubMed: 22555377]
6. Kim S, Lee H, Chung M, Jeon NL. Lab Chip. 2013; 13(8):1489. [PubMed: 23440068]
7. Zheng Y, Chen J, Craven M, Choi NW, Totorica S, Diaz-Santana A, Kermani P, Hempstead B, Fischbach-Teschl C, López JA. Proc. Natl. Acad. Sci. U. S. A. 2012; 109(24):9342. [PubMed: 22645376]
8. Hsu YH, Moya ML, Hughes CC, George SC, Lee AP. Lab Chip. 2013; 13(1):81. [PubMed: 23090158]
9. Hsu YH, Moya ML, Hughes CC, George SC, Lee AP. Lab Chip. 2013; 13(15):2990. [PubMed: 23723013]
10. Yeon JH, Ryu HR, Chung M, Hu QP, Jeon NL. Lab Chip. 2012; 12(16):2815. [PubMed: 22767334]
11. Chen MB, Whisler JA, Jeon JS, Kamm RD. Integr. Biol. 2013; 5(10):1262.
12. Huang CP, Lu J, Seon H, Lee AP, Flanagan LA, Kim HY, Putnam AJ, Jeon NL. Lab Chip. 2009; 9(12):1740. [PubMed: 19495458]
13. Au AK, Lai H, Utela BR, Folch A. Micromachines. 2011; 2(2):179.
14. Moya ML, Hsu YH, Lee AP, Hughes CC, George SC. Tissue Eng. Part C. 2013; 19(9):730.
15. Wang X, Phan DT, Sobrino A, George SC, Hughes CC, Lee AP. Lab Chip. 2016; 16(2):282. [PubMed: 26616908]
16. Rhee M, Light YK, Yilmaz S, Adams PD, Saxena D, Meagher RJ, Singh AK. Lab Chip. 2014; 14((23):4533. [PubMed: 25270338]
17. Oh KW, Lee K, Ahn B, Furlani EP. Lab Chip. 12(3):515. [PubMed: 22179505]
18. Beebe DJ, Mensing GA, Walker GM. Annu. Rev. Biomed. Eng. 2002; 4(1):261. [PubMed: 12117759]
19. Cho H, Kim HY, Kang JY, Kim TS. J Colloid Interface Sci. 2007; 306(2):379. [PubMed: 17141795]
20. Zervantonakis IK, Hughes-Alford SK, Charest JL, Condeelis JS, Gertler FB, Kamm RD. Proc. Natl. Acad. Sci. U. S. A. 2012; 109(34):13515. [PubMed: 22869695]

21. Melero-Martin JM, Khan ZA, Picard A, Wu X, Paruchuri S, Bischoff J. Blood. 2007; 109(11): 4761. [PubMed: 17327403]
22. Moya ML, Hsu Y-H, Lee AP, Hughes CCW, George SC. Tissue Eng. 2013; 19(9):730.
23. Alonzo LF, Moya ML, Shirure VS, George SC. Lab Chip. 2015; 15(17):3521. [PubMed: 26190172]

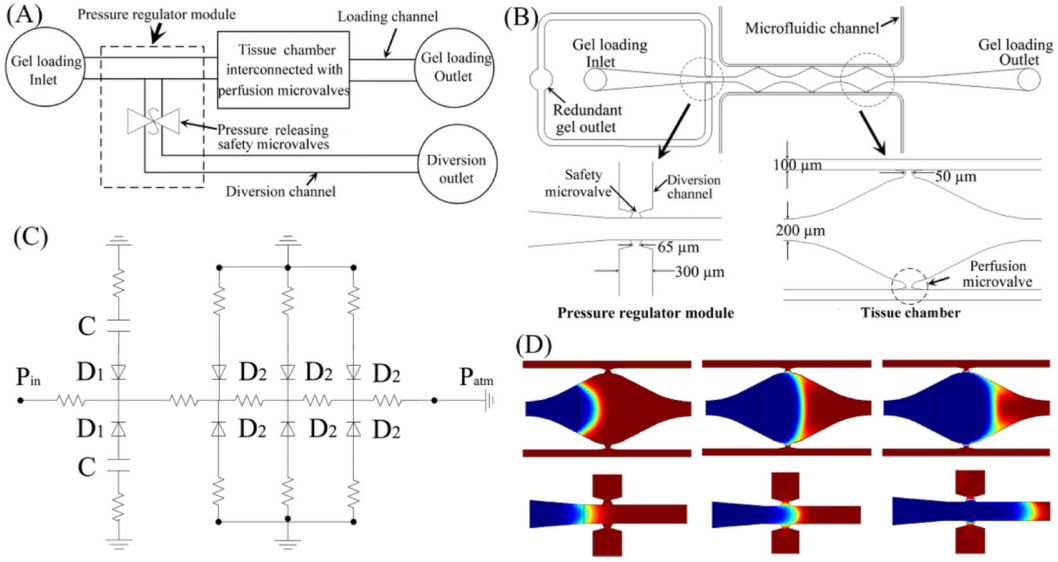

Fig. 1.

Pressure regulator module design. (A) Schematic of basic pressure regulator module structure. (B) Example of one pressure regulator design and its integration into a perfusion-based 3D culture device. (C) A simplified electronic circuit analogy model corresponding to the mechanism of gel loading into the device with pressure regulator module. (D) Simulation results for the gel loading process in both tissue chamber and pressure regulator module without bursting when the hydraulic pressure inside the gel loading channel is less than the burst pressure of their interconnected capillary burst valves. Color scheme: blue represents gel, red represents air and yellow represents gel/air interface.

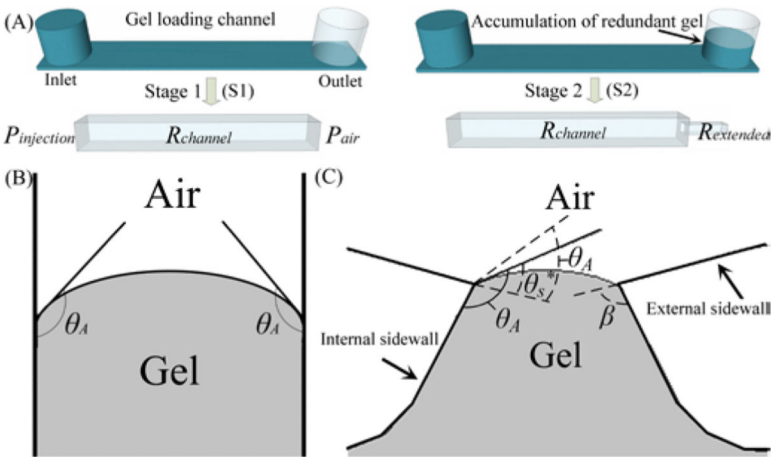

Fig. 2.

(A) Simplified model of gel loading along the microfluidic channel, consisting of two stages. (B) Schematic of gel movement along the loading channel when the contact angles of gel interface with all sidewalls exceed the critical advancing contact angle. (C) Schematic of the capillary burst valve design with gentle slope and different contact angle of gel interface with sidewalls at the vertices.

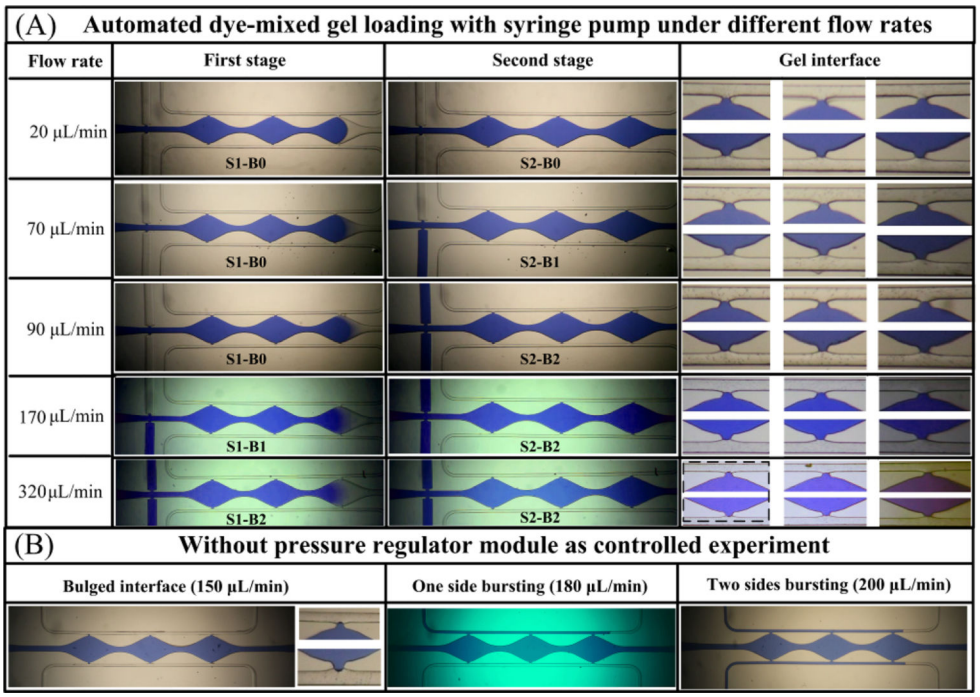

Fig. 3.

(A) Performances of the pressure regulator at two stages by automated dye-mixed gel loading with syringe pump under different flow rates, and a well-controlled gel interface positioned at vertices of the perfusion microvalves. Dashed rectangle in gel interface column represents the slightly bulged gel interface at the high flow rate of 320μL/min. (B) Control experiment using the same gel loading channel without the pressure regulator module.

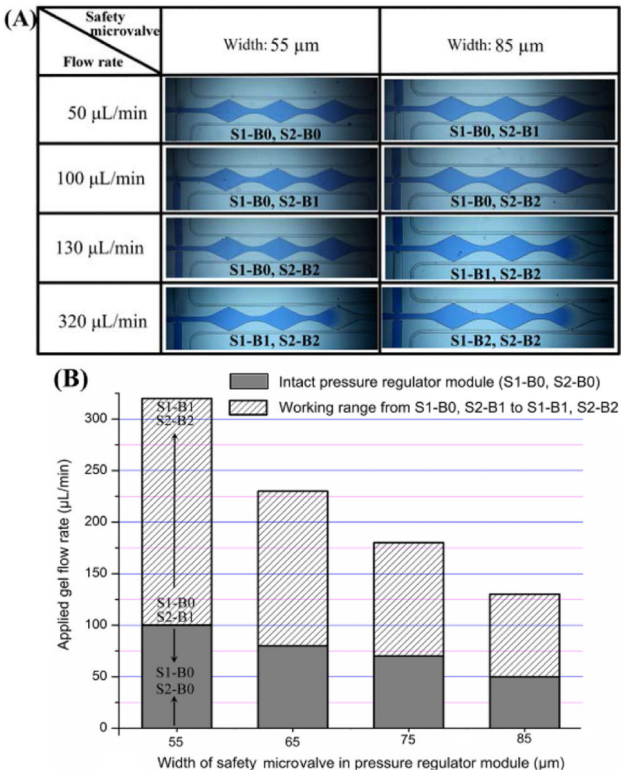

Fig. 4.

(A) Experimental results on dye-mixed gel loading using 55μm and 85μm wide safety microvalves at different flow rates. (B) Comparison results for sensitivity and working range of the pressure regulator with different widths. The narrow safety microvalve has a large working range, while wide safety microvalves have high sensitivity.

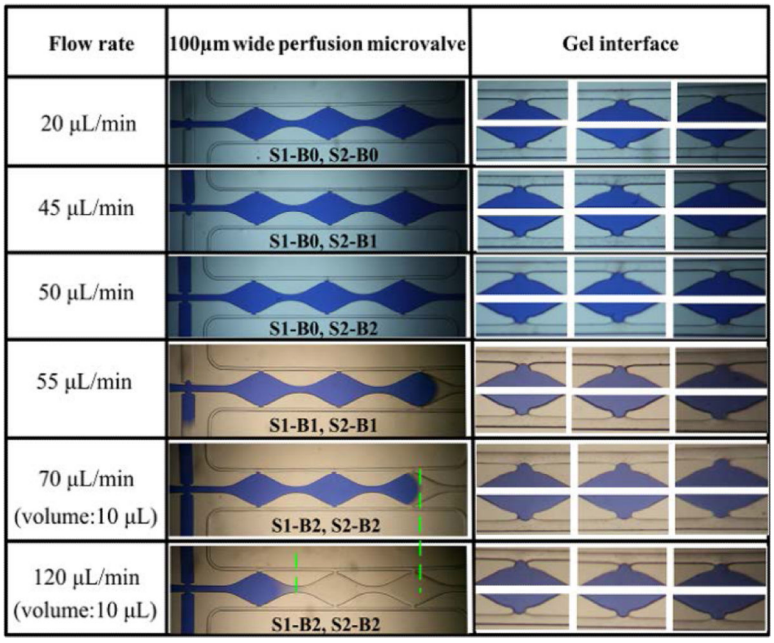

Fig. 5.

Gel confinement with a 100 μm wide perfusion microvalve. Both the pressure regulator module and the gel interface at the perfusion microvalve were sensitive to the applied flow rate. At higher flow rates, smaller gel volumes (e.g. 10μL) could effectively prevent gel bursting from the perfusion microvalve with a wide opening.

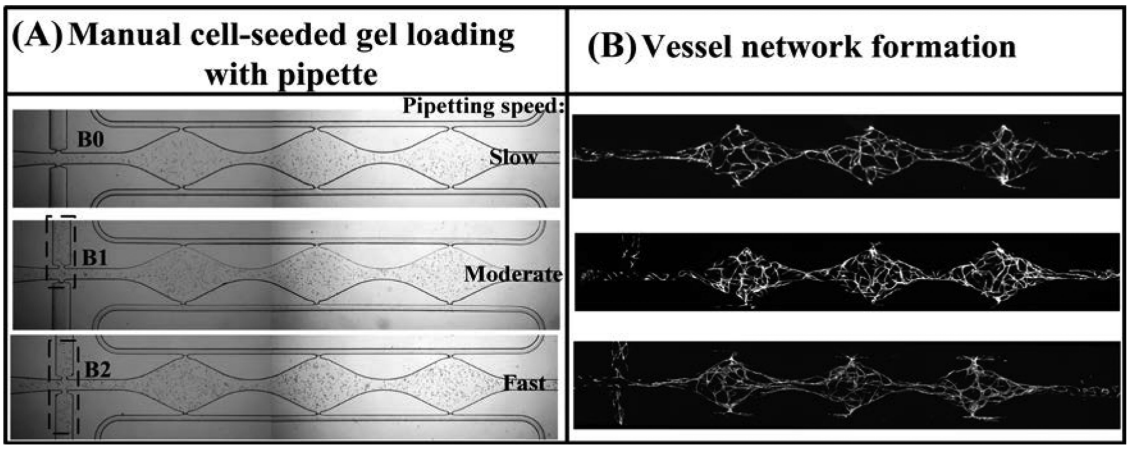

Fig. 6.

(A) Experimental results on manual cell-seeded fibrinogen gel loading with micropipettor under different pipetting speed. B0: no safety microvalve bursting, B1: bursting of one safety microvalve, and B2: bursting of two safety microvalves. Dashed rectangle represents the gel bursting region inside the pressure regulator module. (B) Corresponding vessel network formation inside the microfluidic device after 7 days in culture.

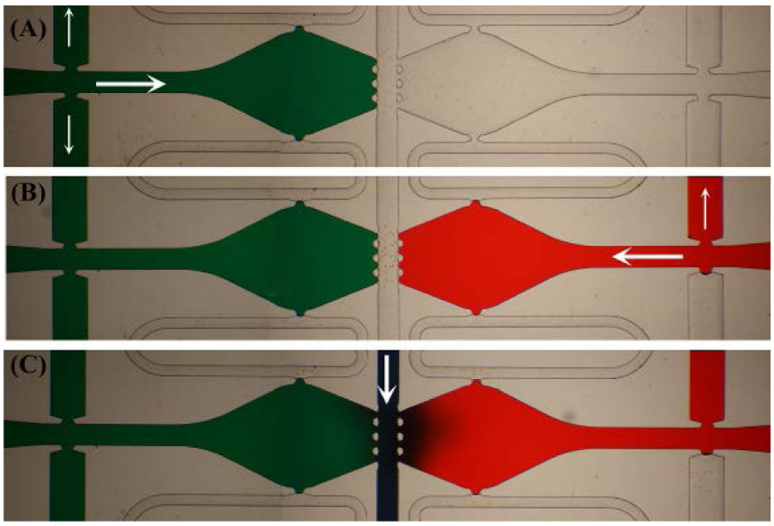

Fig. 7.

Heterotypic dye-mixed gel loading into a microfluidic device with a pressure regulator module at each end serving as a gel loading outlet. (A) Step 1: green dye-mixed gel loading into left chamber and bursting of two safety microvalves. (B) Step 2: red dye-mixed gel loading into right chamber and bursting of only one safety microvalve. (C) Step 3: blue dye-mixed gel loading into central connecting channel to connect the two (green and red) chambers. Diffusion between the chambers then occurred.